

Figure 7 Simulated gain of the proposed antenna

Figure 6 presents the simulated radiation patterns of the proposed design including the vertical ($E\theta$) and horizontal ($E\phi$) polarizations in the H -plane (xz -plane) and E -plane (yz -plane) when operating at 1.8 and 5.2 GHz for GSM and Wi-Fi applications. For the vertical polarization, it can be seen that the radiation patterns in the H -plane are “8”-shaped at 1.8 GHz and nearly omnidirectional at 5.2 GHz band. The simulated peak antenna gains against two frequency bands are shown in Figure 7. For the 1.5–2.2 GHz band, the peak gain is about 2.45 dBi and for the 4.2–6 GHz band the peak gain of about 2.8 dBi is observed.

4. CONCLUSION

A compact printed monopole antenna with multiple rectangular DGS has been presented and investigated through simulated and measured results. Double-resonance is achieved by feeding the antenna with a cross-shaped feed line. The proposed antenna has an impedance bandwidth of about 32% at 1.8 GHz and 29% at 5.2 GHz. A size reduction of about 12% has been achieved, with respect to the similar antenna without the DGS. Acceptable E -plane and H -plane radiation patterns and a peak antenna gain of about 2.8 dBi have been achieved. Experimental results show that the proposed antenna could be a good candidate for both Wi-Fi and GSM applications.

REFERENCES

1. C.A. Balanis, *Antenna theory: Analysis and design*, 3rd ed., Wiley, Hoboken, NJ, 2005.
2. D. Guha and Y.M.M. Antar, *Microstrip and printed antennas: New Trends, techniques and applications*, Wiley, Chichester, West Sussex, UK, 2011.
3. J.-S. Lim, J.-S. Park, Y.-T. Lee, D. Ahn, and S. Nam, Application of defected ground structure in reducing the size of amplifiers, *IEEE Microwave Wireless Compon Lett* 12 (2002), 261–263.
4. J.K. Xiao and Y.F. Zhu, New U-shaped DGS bandstop filters, *Prog Electromagn Res C* 25 (2012), 179–191.
5. L.H. Weng, Y.C. Guo, X.W. Shi, and X.Q. Chen, An overview on defected ground structure, *Prog Electromagn Res B* 7 (2008), 173–189.
6. K.H. Chiang and K.W. Tam, Microstrip monopole antenna with enhanced bandwidth using defected ground structure, *IEEE Antennas Wireless Propag Lett* 7 (2008), 532–535.
7. R. Zaker, C. Ghobadi, and J. Nourinia, Bandwidth enhancement of novel compact single and dual band-notched printed monopole

antenna with a pair of L-shaped slots, *IEEE Trans Antennas Propag* 57 (2009), 3978–3983.

8. Y.-C. Lee, J.-S. Sun, M.-H. Hsu, and R.-H. Chen, A new printed slot loop antenna with tunable strips for 2.4 and 5-GHz wireless applications, *IEEE Antennas Wireless Propag Lett* 8 (2009), 356–358.
9. W.-C. Liu, C.-M. Wu, and Y. Dai, Design of triple-frequency microstrip-fed monopole antenna using defected ground structure, *IEEE Trans Antennas Propag* 59 (2011), 2457–2463.
10. A.K. Arya, A. Patnaik, and M.V. Kartikeyan, Microstrip patch antenna with skew-f shaped DGS for dual band operation, *Prog Electromagn Res M* 19 (2011), 147–160.
11. D. Guha, S. Biswas, M. Biswas, J.Y. Siddiqui, and Y.M.M. Antar, Concentric ring-shaped defected ground structures for microstrip applications, *IEEE Antennas Wireless Propag Lett* 5 (2006) 402–405.
12. Available at: <http://www accuratcircuits.in>.

© 2015 Wiley Periodicals, Inc.

LOW-PROFILE DUAL-WIDEBAND DUAL-INVERTED-L OPEN-SLOT ANTENNA FOR THE LTE/WWAN TABLET DEVICE

Kin-Lu Wong and Pei-Rong Wu

Department of Electrical Engineering, National Sun Yat-sen University, Kaohsiung 80424, Taiwan; Corresponding author: wongkl@ema.ee.nsysu.edu.tw

Received 27 December 2014

ABSTRACT: A low-profile open-slot antenna for the LTE/WWAN operation in the tablet device, such as a smartphone or tablet computer is presented. The antenna consists of two inverted-L (IL) open slots, with one longer IL open slot for the low band of 698–960 MHz and one shorter IL open slot for the high band of 1710–2690 MHz, and is referred to as a dual-inverted-L open-slot antenna in this study. The open ends of the longer and shorter IL open slots face each other and are disposed at the top or bottom edge of the tablet device. Between the two open ends, there is a protruded ground suitable for accommodating electronic elements, such as a USB connector or a camera lens. The antenna shows a low profile of 7 mm to the top or bottom edge and is excited by two feeds, with the first and second feeds, respectively, exciting the longer and shorter IL open slots thereof. By aided with the wideband matching circuits in the first and second feeds, the antenna can provide two wide operating bands covering the 698–960 and 1710–2690 MHz bands. Easy control of the two feeds for the desired dual-wideband operation is also obtained. The antenna is suitable for dual-wideband LTE operation in the modern tablet device, especially for the tablet device with a narrow spacing between the display panel and the top or bottom edge thereof. © 2015 Wiley Periodicals, Inc. *Microwave Opt Technol Lett* 57:1813–1818, 2015; View this article online at wileyonlinelibrary.com. DOI 10.1002/mop.29204

Key words: mobile antennas; open slot antennas; slot antennas; tablet device antennas; LTE/WWAN antennas

1. INTRODUCTION

Recently, to achieve better appearance of the modern tablet device, such as a smartphone or tablet computer, the spacing between the display panel and the top or bottom edge of the casing thereof is becoming very narrow. The narrow spacing (usually less than 10 mm) causes a great challenge on the design of the internal antenna therein, especially for the antenna to cover the LTE/WWAN operation (698–960/1710–2690 MHz). It

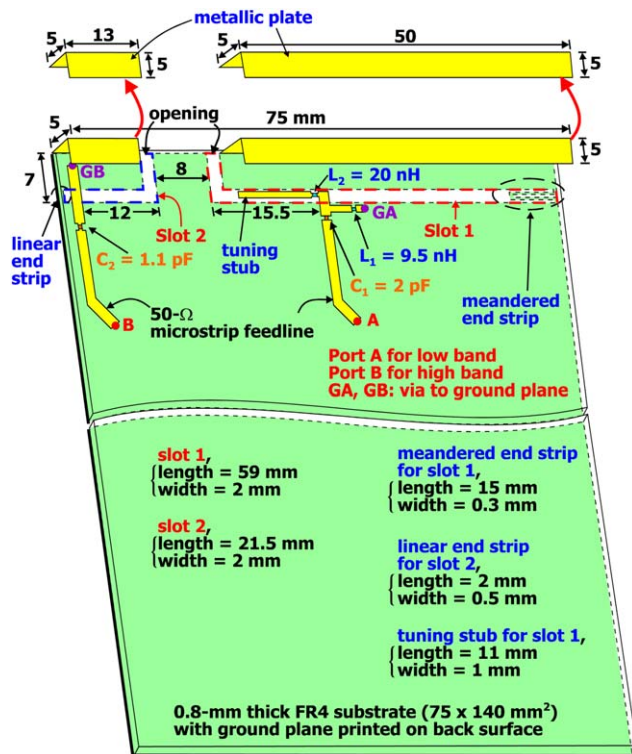


Figure 1 Geometry of the dual-inverted-L open-slot antenna for the LTE/WWAN tablet device. [Color figure can be viewed in the online issue, which is available at wileyonlinelibrary.com]

is also noted that there are very few reported LTE/WWAN antennas having a low profile of less than 10 mm [1,2]. For the recently reported antennas in Ref 1,2, their antenna profile is as low as 8 mm only, and their operating bandwidths can cover the 698–960 and 1710–2690 MHz bands. To achieve such a low profile with dual-wideband operation, a coupled-fed loop structure is applied in [2], while a two-strip monopole antenna formed by a driven strip and a shorted parasitic strip is applied in [1].

In this article, different to the monopole or loop antenna applied in [1,2], we demonstrate an open-slot antenna structure to achieve a very low profile of 7 mm to cover the 698–960 and 1710–2690 MHz bands in the tablet device. The proposed antenna consists of two inverted-L (IL) open slots, with one longer IL open slot for the low band of 698–960 MHz and one shorter IL open slot for the high band of 1710–2690 MHz. The antenna is referred to as a dual-inverted-L open-slot antenna in

this study. The antenna is also configured to have its two open ends disposed at the top or bottom edge of the tablet device. As there are no open ends at the two long side edges of the tablet device, the effects of the user's hand holding the tablet device on the antenna performance can be greatly decreased. In addition, the antenna is also configured to have a protruded ground between the two open ends, which allows the antenna to easily integrate with nearby electronic elements such as a USB connector or a camera lens [3].

The antenna is excited by using two feeds, with the first and second feeds, respectively, exciting the longer and shorter IL open slots thereof. The two open slots are excited to contribute their quarter-wavelength resonant slot modes [4–8], respectively, in the desired low and high bands. By aided with the wideband matching circuits in the two feeds, the antenna can provide a dual-wideband operation to cover the 698–960 and 1710–2690 MHz bands. Detailed configuration of the proposed antenna is described, and its operating principle is discussed. The simulation and experimental results are also presented.

2. PROPOSED ANTENNA

2.1. Antenna Structure

The geometry of the proposed dual-inverted-L open-slot antenna for the LTE/WWAN tablet device is shown in Figure 1. In this study, the tablet device is considered to be a 5.5-inch smartphone, with a system ground plane of size $75 \times 140 \text{ mm}^2$. The ground plane is printed on a 0.8-mm thick FR4 substrate of relative permittivity 4.4 and loss tangent 0.02. The antenna consists of two IL open slots and is disposed at the top edge of the system ground plane with a low profile of 7 mm. Note that the antenna can also be disposed at the bottom edge of the system ground plane in practical applications [9], or two such antennas can be disposed, respectively, at the top and bottom edges of the system ground plane for the LTE multi-input multi-output (MIMO) operation [10–12].

To more clearly demonstrate the proposed antenna, the photos of the fabricated antenna are presented in Figure 2. The antenna's low and high bands are respectively contributed by the longer IL open slot (slot 1 in the figure) and the shorter IL open slot (slot 2 in the figure). The first feed at port A excites slot 1, while the second feed at port B excites slot 2. Note that the open ends of slot 1 and 2 are at the top edge, and there is a protruded ground of width 8 mm between the two open ends. The protruded ground can be used to accommodate nearby electronic elements [13]. Two metallic plates of height 5 mm and width 5 mm are also added and connected to the system ground plane. The added metallic plates are helpful in achieving good excitation of the slot modes contributed by slot 1 and 2, thereby

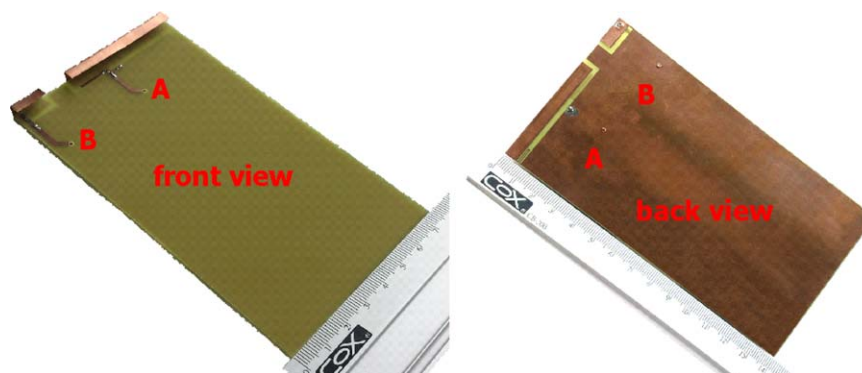


Figure 2 Photos of the fabricated antenna. [Color figure can be viewed in the online issue, which is available at wileyonlinelibrary.com]

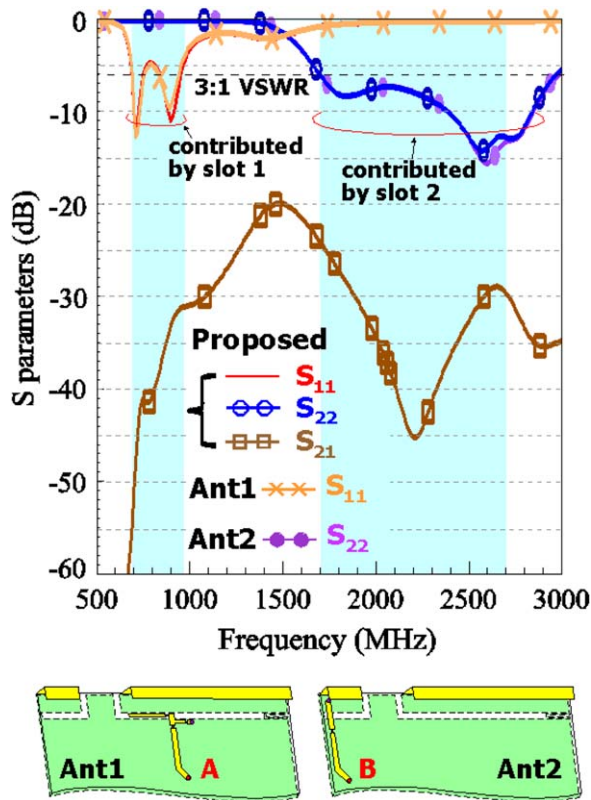


Figure 3 Simulated S -parameters for the proposed antenna, the case with the first feed only (Ant1), and the case with the second feed only (Ant2). [Color figure can be viewed in the online issue, which is available at wileyonlinelibrary.com]

leading to wider bandwidths for the antenna [14]. It is also noted that for practical applications, the metallic plates are promising to be printed or disposed on the inner surface of the casing of the smartphone, leading to compact integration of the antenna within the smartphone.

Slot 1 has a length of 59 mm and a width of 2 mm. Although the length of slot 1 is only about 0.14 wavelength at 700 MHz, slot 1 can generate its fundamental (0.25-wavelength) slot mode [6,15,16] in the desired low band. The decrease in the required resonant slot length is partly owing to the FR4 substrate loading and partly owing to the use of the meandered end strip at the closed end of the slot. The meandered end strip has a length of 15 mm and a width of 0.3 mm and can lead to an increased resonant path for the excited surface current around the closed end of the slot, thereby decreasing the fundamental resonant frequency of the slot. Detailed effects of the meandered end strip will be discussed in Section 2.2 with the aid of Figure 5.

The first feed at port A includes an inductor-loaded tuning stub of length 11 mm and a high-pass matching circuit formed by a parallel inductor L_1 (9.5 nH) and a series capacitor C_1 (2 pF). The tuning stub has a narrow width of 1 mm. It is aligned inside and parallel to the longer IL open slot. The inductor loaded in the tuning stub has an inductance of 20 nH (L_2) and can lead to improve impedance matching of the excited resonant mode of slot 1. The high-pass matching circuit further leads to a dual-resonance excitation [17,18] of the excited slot mode, hence providing a wide low band for the antenna to cover the 698–960 MHz band. The circuit elements L_1 , C_1 , and L_2 form as a wideband matching circuit for the first feed and will be discussed in detail with the aid of Figure 6 in Section 2.3.

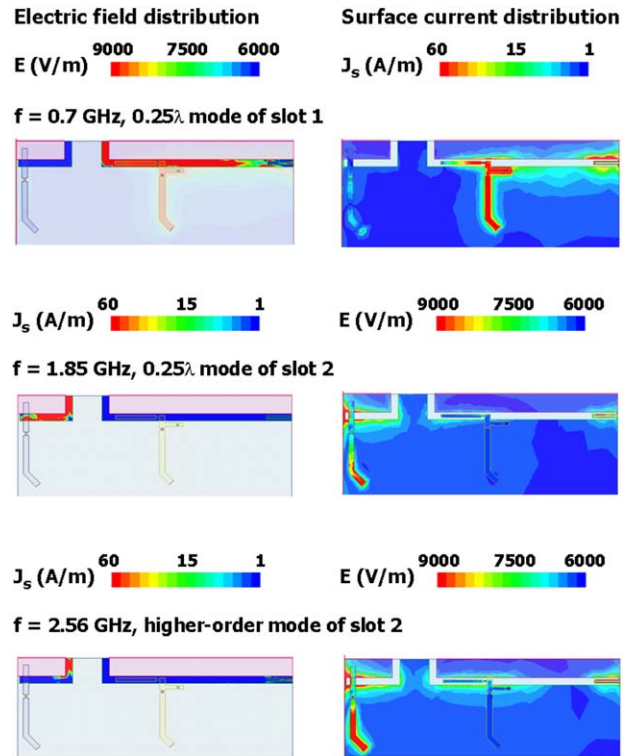


Figure 4 Simulated electric field and surface current distributions for the antenna. [Color figure can be viewed in the online issue, which is available at wileyonlinelibrary.com]

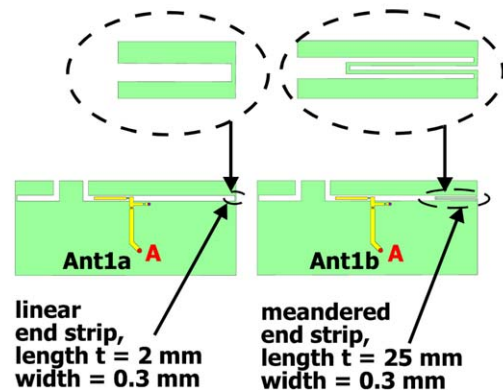
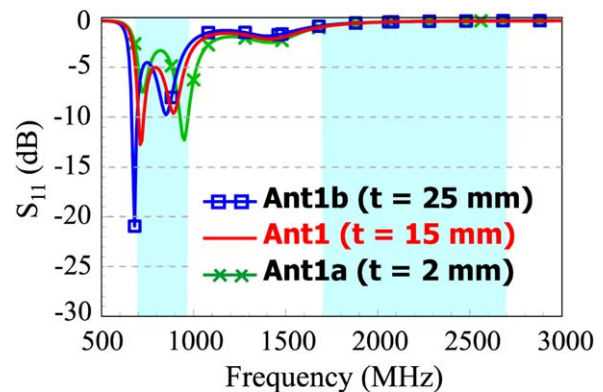
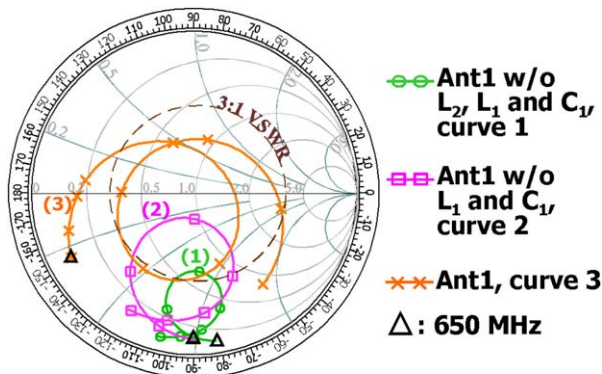


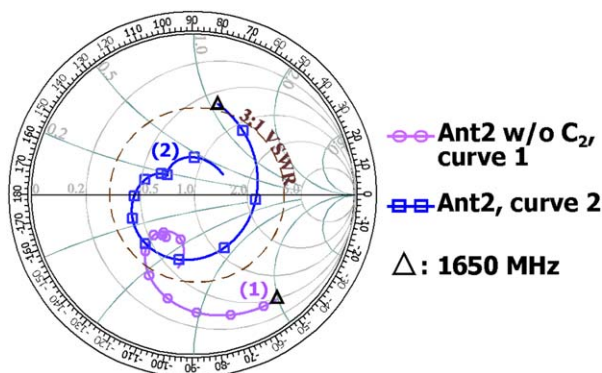
Figure 5 Simulated S_{11} for Ant1 with various end-connecting strips at the closed end of slot 1. [Color figure can be viewed in the online issue, which is available at wileyonlinelibrary.com]



Frequency range : 650~1000 MHz
Interval between two marks: 50 MHz

Figure 6 Simulated input impedance on the Smith chart for Ant1 without the circuit elements of L_1 , C_1 , and L_2 (curve 1), Ant1 without the circuit elements of L_1 and C_1 (curve 2), (curve 1), and Ant1 (curve 3) in the frequency range of 650–1000 MHz. [Color figure can be viewed in the online issue, which is available at wileyonlinelibrary.com]

Slot 2 has a length of 21.5 mm and a width of 2 mm. Similarly, although the length of slot 2 is only about 0.14 wavelength at 1.9 GHz, slot 2 can generate its fundamental (0.25-wavelength) slot mode in the desired high band. Also note that at the closed end of slot 2, a simple linear end strip of width 0.5 mm and length 2 mm is found to be sufficient for slot 2 to contribute its fundamental slot mode in the desired high band. For feeding slot 2, the second feed at port B uses a shorted tuning stub (see the point GB in the figure) and has an embedded series capacitor C_2 (1.1 pF). By terminating the tuning stub to the ground plane, the length of the tuning stub can be decreased. In this case, an added series capacitor can lead to good excitation of the fundamental slot mode and its higher-order slot mode as well. The two slot modes can also be combined into a wide operating band for the antenna's high band to cover the 1710–2690 MHz band. Effects of the second feed on achieving the wide high band are discussed in detail with the aid of Figure 7 in Section 2.3.



Frequency range : 1650~2750 MHz
Interval between two marks: 100 MHz

Figure 7 Simulated input impedance on the Smith chart for Ant2 without the circuit element of C_2 (curve 1) and Ant2 (curve 2) in the frequency range of 1650–2750 MHz. [Color figure can be viewed in the online issue, which is available at wileyonlinelibrary.com]

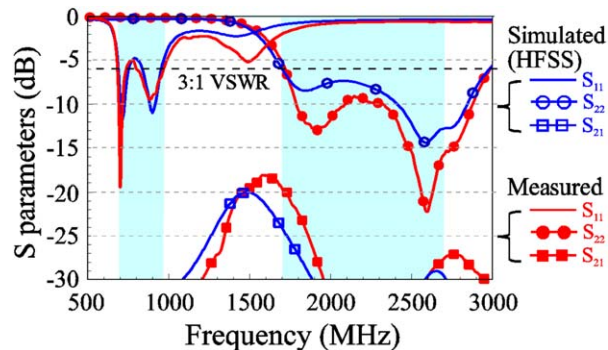


Figure 8 Measured and simulated S -parameters for the fabricated antenna. [Color figure can be viewed in the online issue, which is available at wileyonlinelibrary.com]

2.2. Operating Principle

The antenna's low and high bands can be, respectively, controlled by the first and second feeds. Good isolation between the two feeds can also be obtained. The simulated S -parameters for the proposed antenna, the case with the first feed only (Ant1), and the case with the second feed only (Ant2) are presented in Figure 3. The simulated results are obtained using the full-wave electromagnetic field simulator HFSS version 15 [19]. The S_{11} and S_{22} are the reflection coefficients seen at port A for slot 1 excitation and at port B for slot 2 excitation, respectively. The S_{21} is the transmission coefficient between port A and B. The results show that the two wide bands of the proposed antenna are contributed, respectively, by Ant1 and Ant2. The desired low and high bands for the LTE/WWAN operation are shown as shaded regions in the figure. The isolation between two ports is also seen to be less than about 31 dB in the low band and less than about 24 dB in the high band. Note that the impedance matching in the low and high bands is generally less than -6 dB (3:1 VSWR), except for some frequencies in the low band less than about -5 dB. However, the measured antenna efficiency including the mismatching losses (will be shown in Figure 9) is all better than 40% in the low band, which is acceptable for practical applications [20,21].

Figure 4 shows the simulated electric field and surface current distributions for the antenna. The results for three representative frequencies at 0.7, 1.85, and 2.56 GHz are shown. At 0.7 GHz, strong electric fields at the opening of slot 1 are seen, while at 1.85 and 2.56 GHz, strong electric fields at the opening of slot 2 are seen. The excited surface currents along two

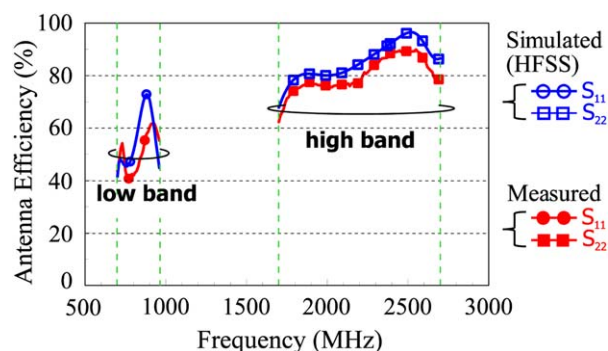


Figure 9 Measured and simulated antenna efficiencies for the fabricated antenna. [Color figure can be viewed in the online issue, which is available at wileyonlinelibrary.com]

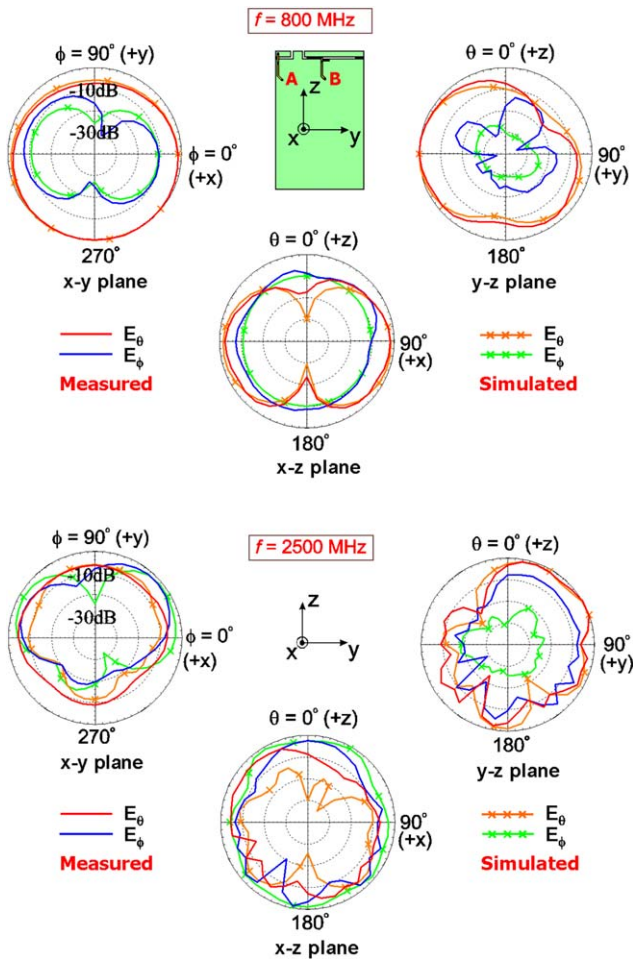


Figure 10 Measured and simulated radiation patterns for the fabricated antenna. [Color figure can be viewed in the online issue, which is available at wileyonlinelibrary.com]

parallel edges of the excited slots at the three frequencies are also observed to be about symmetric. The observed electric field and surface current distributions indicate that the slot resonant modes are excited. As discussed in Section 2.1, the resonant modes at 0.7 and 1.85 GHz are, respectively, the fundamental (0.25-wavelength) resonant modes of slot 1 and 2, and the resonant mode at 2.56 GHz is a higher-order resonant mode contributed by slot 2.

Effects of the meandered end strip disposed at the closed end of slot 1 are also studied. Figure 5 shows the simulated S_{11} for Ant1 with various end-connecting strips at the closed end of slot 1. Ant1 is with a 15-mm meandered end strip, while Ant1a is with a simple linear end strip of 2 mm and Ant1b is with a meandered end strip of 25 mm. It is seen that the operating band is shifted to lower frequencies with an increase in the length of the end-connecting strip. This is mainly because the meandered end strip can lengthen the resonant path of the excited surface currents around the closed end of slot 1, which in turn increases the effective resonant length of the excited slot mode and decreases the resonant frequency thereof.

2.3. Wideband Matching Circuits for the Two Feeds

The wideband operation of the antenna's low and high bands is aided by the wideband matching circuits for the first and second feeds of the antenna. Figure 6 shows the simulated input imped-

ance on the Smith chart for Ant1 without the circuit elements of L_1 , C_1 , and L_2 (curve 1), Ant1 without the circuit elements of L_1 and C_1 (curve 2), and Ant1 (curve 3) in the frequency range of 650–1000 MHz. In the matching circuit for the first feed, the inductor L_2 is embedded in the tuning stub of the microstrip feedline to improve the impedance matching of the excited resonant mode of slot 1. The capacitor C_1 and the inductor L_1 are formed as a high-pass matching circuit for achieving dual-resonance excitation of the excited slot mode. From the results of curve 1, it is seen that a resonant mode is excited; however, the impedance matching of the excited resonant mode is poor. With the presence of L_2 , the impedance matching of the excited resonant mode can be improved (see curve 2 vs. curve 1). By further adding the high-pass circuit of C_1 and L_1 , a dual-resonance of the excited resonant mode is seen (see curve 3), which can cover the desired low band (698–960 MHz).

The second feed for generating the wide high band is also analyzed. Figure 7 shows the simulated input impedance on the Smith chart for Ant2 without the circuit element of C_2 (curve 1) and Ant2 (curve 2) in the frequency range of 1650–2750 MHz. As described in Section 2.1, the second feed uses a shorted tuning stub and a series capacitor C_2 . When the capacitor C_2 is not present, a resonant mode can be excited (see curve 1), however, the impedance matching is not acceptable for the entire desired high band (1710–2690 MHz). By simply adding the capacitor C_2 , it is seen that the excited slot mode can have much improved impedance matching (see curve 2). This suggests that the use of a shorted tuning stub and a series capacitor together can result in a good excitation of the slot resonant mode. In addition, both the fundamental and higher-order resonant modes of slot 2 (see the two resonant frequencies at 1.85 and 2.56 GHz studied in Fig. 4) are excited with good impedance matching and formed into the wide high band for the antenna.

3. EXPERIMENTAL RESULTS

The proposed antenna was fabricated and tested, and the photos of the fabricated antenna are shown in Figure 2. The measured and simulated S parameters for the fabricated antenna are presented in Figure 8. The results confirm the agreement between the measurement and simulation. The antenna provides two wide operating bands with acceptable impedance matching of better than about 3:1 VSWR. The measured isolation between the two feeds is also seen to be less than about -19 dB in the high band. For the low band, the measured isolation is less than -30 dB and is not shown in the figure.

Figure 9 shows the measured and simulated antenna efficiencies. The antenna's radiation performance is measured in a far-field anechoic chamber. The obtained results also confirm agreement of the measured data and the simulated results. The measured antenna efficiency includes the mismatching losses and is about 40–62% in the low band and about 62–90% in the high band. The obtained antenna efficiency is acceptable for mobile communication applications.

The measured and simulated radiation patterns at 800 and 2500 MHz are plotted in Figure 10. At 800 MHz, a representative frequency in the low band, near-omnidirectional radiation in the x - y plane is seen. This indicates that the system ground plane also contributes to the radiation in the low band. In the x - z plane (elevation plane orthogonal to the system ground plane), symmetric radiation pattern is generally seen. While in the y - z plane (elevation plane parallel to the system ground plane), stronger radiation in the $-y$ direction is seen. This is largely

related to the slot opening, where strong electric fields occur, disposed to the left-hand side of slot 1.

At 2500 MHz, a representative frequency in the high band, stronger radiation to the +y direction in the x-y plane and y-z plane is seen. This is different from that observed at 800 MHz, and is largely related the slot opening disposed to the right-hand side of slot 2. In the x-z plane, however, symmetric radiation pattern is also generally seen as that observed at 800 MHz.

4. CONCLUSION

A low-profile (7 mm only) open-slot antenna for the tablet device application has been proposed and studied. The antenna is capable of providing two wide operating bands for the LTE/WWAN operation in the 698–960/1710–2690 MHz bands. The antenna uses two IL open slots and two feeds with wideband matching circuits. Owing to its low profile, the antenna is promising to be disposed in a narrow spacing between the display panel and the top or bottom edge of the tablet device. The operating principle of the proposed antenna to generate two wide operating bands has been presented. Acceptable radiation characteristics of the antenna for mobile communication applications have also been obtained.

REFERENCES

1. K.L. Wong and T.W. Weng, Very-low-profile dual-wideband tablet device antenna for LTE/WWAN operation, *Microwave Opt Technol Lett* 56 (2014), 1938–1942.
2. K.L. Wong and M.T. Chen, Very-low-profile dual-wideband loop antenna for LTE tablet computer, *Microwave Opt Technol Lett* 57 (2015), 141–146.
3. K.L. Wong, P.W. Lin, and C.H. Chang, Simple printed monopole slot antenna for penta-band WWAN operation in the mobile handset, *Microwave Opt Technol Lett* 53 (2011), 1399–1404.
4. H. Wang, M. Zheng, and S.Q. Zhang, Monopole slot antenna, U.S. Patent 6,618,020 B2, 2003.
5. P.L. Sun, H.K. Dai, and C.H. Huang, Dual band slot antenna with single feed line, U.S. Patent 6,677,909 B2, 2004.
6. C.I. Lin and K.L. Wong, Printed monopole slot antenna for internal multiband mobile phone antenna, *IEEE Trans Antennas Propag* 55 (2007), 3690–3697.
7. Z. Liu and K. Boyle, Bandwidth enhancement of a quarter-wavelength slot antenna by capacitive loading, *Microwave Opt Technol Lett* 51 (2009), 2114–2116.
8. K.L. Wong and L.C. Lee, Multiband printed monopole slot antenna for WWAN operation in the laptop computer, *IEEE Trans Antennas Propag* 57 (2009), 324–330.
9. Y.W. Chi and K.L. Wong, Quarter-wavelength printed loop antenna with an internal printed matching circuit for GSM/DCS/PCS/UMTS operation in the mobile phone, *IEEE Trans Antennas Propag* 57 (2009), 2541–2547.
10. W. Dou, S. Senatore, and A. Zarnowitz, Internal diversity antenna architecture, U.S. Patent 7,940,223 B2, 2011.
11. V. Plicanic, B.K. Lau, A. Derneryd, and Z. Ying, Actual diversity performance of a multiband diversity antenna with hand and head effects, *IEEE Trans Antennas Propag* 57 (2009), 1547–1556.
12. K.L. Wong, T.W. Kang, and M.F. Tu, Internal mobile phone antenna array for LTE/WWAN and LTE MIMO operations, *Microwave Opt Technol Lett* 53 (2011), 1569–1573.
13. K.L. Wong, W.Y. Chen, and T.W. Kang, On-board printed coupled-fed loop antenna in close proximity to the surrounding ground plane for penta-band WWAN mobile phone, *IEEE Trans Antennas Propag* 59 (2011), 751–757.
14. Z. Liu and K. Boyle, Antenna arrangement and a radio apparatus including the antenna arrangement, U.S. Patent 8,638,266 B2, 2014.
15. K.L. Wong and W.J. Lin, WWAN/LTE printed slot antenna for tablet computer application, *Microwave Opt Technol Lett* 54 (2012), 44–49.

16. F.H. Chu and K.L. Wong, Simple folded monopole slot antenna for penta-band clamshell mobile phone application, *IEEE Trans Antennas Propag* 57 (2009), 3680–3684.
17. K.L. Wong and L.Y. Chen, Small-size LTE/WWAN tablet device antenna with two hybrid feeds, *IEEE Trans Antennas Propag* 62 (2014), 2926–2934.
18. K.L. Wong and C.Y. Tsai, Small-size stacked inverted-F antenna with two hybrid shorting strips for the LTE/WWAN tablet device, *IEEE Trans Antennas Propag* 62 (2014), 3962–3969.
19. ANSYS high frequency structure synthesizer (HFSS), Pittsburgh, PA, Available at <http://www.ansys.com/products/hf/hfss/>
20. K.L. Wong and M.T. Chen, Small-size LTE/WWAN printed loop antenna with an inductively coupled branch strip for bandwidth enhancement in the tablet computer, *IEEE Trans Antennas Propag* 61 (2013), 6144–6151.
21. K.L. Wong and T.W. Weng, Small-size triple-wideband LTE/WWAN tablet device antenna, *IEEE Antennas Wireless Propag Lett* 12 (2013), 1516–1519.

© 2015 Wiley Periodicals, Inc.

MINIATURIZED BANDPASS SUBSTRATE INTEGRATED WAVEGUIDE FILTER WITH FREQUENCY-DEPENDENT COUPLING REALIZED USING ASYMMETRIC GCPW DISCONTINUITY

Andrzej Jedrzejewski, Lukasz Szydowski, and Michał Mrozowski

Faculty of Electronics, Telecommunications and Informatics, Gdansk University of Technology, 11/12 Gabriela Narutowicza Street, 80-233 Gdansk, Poland; Corresponding author: andrzej.jedrzejewski87@gmail.com

Received 12 January 2015

ABSTRACT: An asymmetric GCPW discontinuity is proposed to provide frequency-dependent coupling in microwave bandpass filters. Wider and narrow sections introduce, respectively, the capacitive and inductive component to the equivalent circuit representing coupling. By selecting the dimensions of the discontinuity and width of the inductive window in substrate integrated waveguide, an additional transmission zero can be introduced at prescribed positions. A distinct feature of the proposed structure is a small footprint and low loss. As an example, a bandpass filter with a central frequency of 4.6 GHz and a 200 MHz passband is designed, and its performance is measured. © 2015 Wiley Periodicals, Inc. *Microwave Opt Technol Lett* 57:1818–1821, 2015; View this article online at wileyonlinelibrary.com. DOI 10.1002/mop.29203

Key words: substrate integrated waveguide technology; bandpass filters; frequency-dependent coupling; asymmetric GCPW discontinuity; miniaturized filter

1. INTRODUCTION

Substrate integrated waveguide (SIW) [1,2] is a relatively new concept in microwave engineering that has been proposed to overcome the drawbacks of the conventional metallic waveguides, such as large size and weight and at the same time to achieve better performance at higher frequencies than microstrip. The SIW is a type of waveguide that is integrated in the double-side metallized dielectric substrate with two rows of metallized via holes acting as narrow walls of the guide. This construction provides an easy integration with planar circuitry, good shielding, low loss, low-profile, low-cost, and low-weight scheme while maintaining high performance, which is particularly useful for the airborne and satellite system applications.